Organic Process Research & Development **2001**, *5*, 158–166

# Determination of Reaction Parameters Using a Small Calorimeter with an Integrated FT-IR Probe and Parameter Fitting

Jörg Pastré, Andreas Zogg, Ulrich Fischer,* and Konrad Hungerbühler

*Swiss Federal Institute of Technology ETH, Laboratory of Technical Chemistry, Safety and Environmental Technology Group, CH 8092 Zurich, Switzerland*

**Abstract:**

**To identify optimal operating conditions of a chemical process, knowledge on kinetic and thermodynamic parameters of the main reactions is needed. In particular in the fine chemical industry during the early phases of process development this knowledge is usually low. One reason is that only small amounts of substrate are available to perform the required calorimetric and analytical experiments. Therefore, we present in this paper a new prototype reaction calorimeter with a volume of 50 mL. Despite its small volume, the reaction calorimeter is combined with an IR-ATR probe to obtain augmented information from semibatch experiments under isothermal conditions. Furthermore, we present a new method to analyze the calorimetric measurements. The novelty of the approach is that all heat flows in the calorimeter are modeled together with the chemical reaction. For general reaction kinetics this reactor model cannot be solved analytically, and thus, numerical methods are applied for fitting the model parameters to the measurement data. In contrast to the traditional method of thermal conversion the rate constants and the heats of reaction are computed at the same time. The new reaction calorimeter and the new evaluation principle of the thermal signal were both tested using a single-step second-order model reaction. Also the FT-IR data were evaluated by fitting the parameters in the reactor model numerically. The reaction parameters obtained with both measurement techniques are in good agreement with values published in the literature demonstrating the feasibility of the approach.**

## Introduction

To identify the optimal operating conditions of a chemical process (e.g., by modeling using flow-sheeting programs) knowledge on kinetic and thermodynamic parameters, in the following referred to as "reaction parameters", for the most important main and side reactions is needed. In early stages of chemical process development the focus lies on determining scale-up factors and macro-kinetic parameters rather than on gathering in-depth mechanistic insight.

However, a conventional method for investigating a reaction during process development is reaction calorimetry. Reaction calorimeters are used mainly for safety assessments and for understanding most necessary scale-up factors such as heat of reaction and conversion time curves at working temperature.

To gather additional information on a reaction, the reaction calorimeters are often combined with in situ analytical techniques such as FT-IR (Fourier transform infrared) spectroscopy. Combinations of FT-IR with standard reaction calorimeters were already presented in the literature.[1] The calorimetric signal reflects the sum of all physicochemical changes of the reaction system that have an impact on the heat balance of the system, such as, for example, thermal conductivity or a change of viscosity, which result in a change of the heat transfer coefficient and influence the calorimetric signal in addition to the heat produced by the different chemical reactions. The FT-IR measurements on the other hand reflect the sum of all chemical changes of the system, even when the heat production is rather small. The vast amount of chemical information is displayed in the about 2000 wavenumbers recorded.

Unfortunately the reaction calorimeters that can be equipped with an IR probe require a large volume on the order of 200−2000 mL, meaning a considerable consumption of test substance. However, in early stages of process development the available amount of reactants is often small, and thus the use of commercially available reaction calorimeters is impeded. Therefore, we developed a small reaction calorimeter with power compensation, which allows stirring, different dosing profiles, and the combination with an IR dipper.

The traditional way of evaluating the thermal signal is to apply the principle of thermal conversion.[2] In this approach, during the dosing period of a semibatch experiment, the dosing temperature and the heat capacity of the feed have to be known. If heats of mixing appear during the dosing period they have to be determined in a separate experiment. Furthermore, if the reaction is not run until completion, which can take a long time for second-order reactions, the extent of conversion at the end of the experiments has to be determined by another analytical technique such as gas chromatography.

We present a new method to analyze the calorimetric measurements. The novelty of the approach is that all heat flows in the calorimeter are modeled together with the chemical reaction. The reaction model is expressed in terms

(1) (a) Landau, R. N.; McKenzie, P. F.; Forman, A. L.; Dauer, R. R.; Futran, M. *Process Control Qual.* **1995**, *7*, 133. (b) LeBlond, C.; Wang, J.; Larsen, R. D.; Orella, C. J.; Forman, A. L.; Landau, R. N.; Laquidara, J.; Sowa, J. R.; Blackmond, D. G.; Sun, Y.-K. *Thermochim. Acta* **1996**, *289*, 189. (c) LeBlond, C.; Wang, J.; Larsen, R.; Orella, C.; Sunn, Y.-K. *Top. Catal.* **1998**, *5*, 149. (d) am Ende, D. J.; Clifford, P. J.; DeAntonis, D. M.; SantaMaria C.; Brenek, S. J. *Org. Process Res. Dev.* **1999**, *3*, 319. (e) Ubrich, O.; Srinivasan, B.; Lerena, P.; Bonvin, D.; Stoessel, F. *J. Loss Prev. Process Ind.* **1999**, *12*, 485.

(2) am Ende, D. J..; Clifford, P. J.; Northrup, D. L. *Thermochim. Acta* **1996**, *289*, 143.

 10.1021/op000072a CCC: $20.00 
Published on Web 01/31/2001

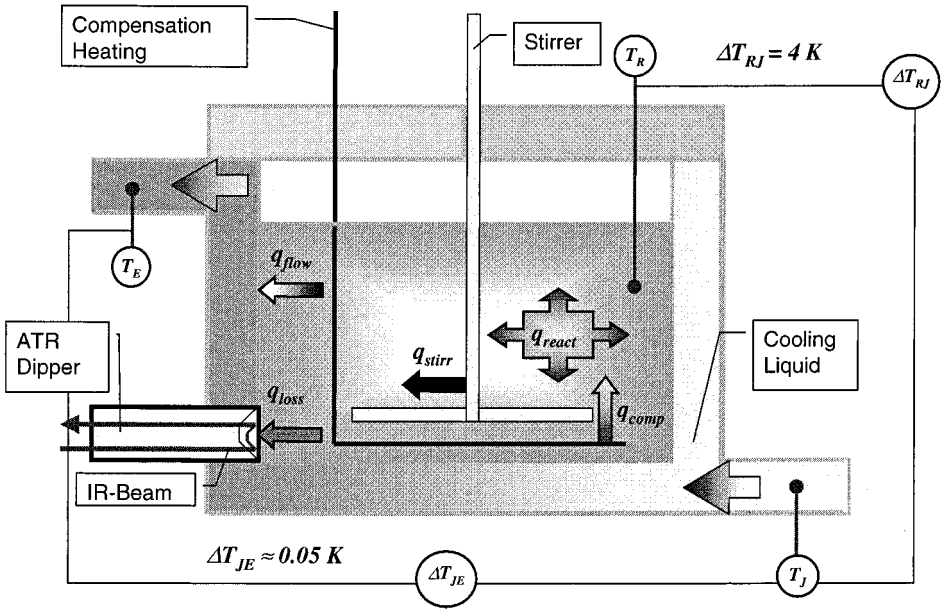


***Figure 1.*** **Principle of power compensation calorimetry and experimental setup. The compensation heating is controlled by a PID-controller. See text and Table 1 for notation.**

of differential equations and comprises the change in volume during dosing. For general reaction kinetics this reactor model cannot be solved analytically, and thus, numerical methods are applied for fitting the model parameters to the measurement data. In contrast to the traditional method of thermal conversion the rate constants and the heats of reaction are computed at the same time.

The new reaction calorimeter and the new evaluation principle of the thermal signal were both tested using a single-step second-order model reaction, for which reference parameters are available in the literature.[3] Also the FT-IR data were evaluated by fitting the parameters in the reactor model numerically. Advantages of the new device and the evaluation approaches are: less substance is needed for the experiments; the temperature and the heat capacity of the feed as well as mixing enthalpies have not to be determined; the duration of the experiments can be shortened; and no calibration of the FT-IR spectrometer was required.

## Material and Methods

**Experimental Setup.** In Figure 1 the calorimetric device is shown schematically. It consists of a small reaction vessel made of glass with a cooling jacket and a lid, the latter being equipped with an electric motor for stirring the reaction mass. The device has a volume of 50 mL and uses the power compensation approach.[4] The vessel is not pressure-proof; therefore, the experiments were done at ambient pressure. The whole calorimeter is placed in an insulated box, which is heated to the temperature of the cooling liquid (silicon oil) in the jacket.

The compensation heating controls the reactor temperature so that it is always 4 K above the jacket temperature. When a reaction proceeds, the power of the compensation heater is reduced by the PID-controller, in dependence of the heat of reaction. Such, a constant heat flow out of the vessel into the jacket is generated as long as the reactor-sided heat transfer coefficient does not change. The power of the compensation heating $q_{comp}$, the reactor temperature $T_R$, the jacket temperature $T_J$, the temperature difference between jacket in- and outlet ($\Delta T_{JE}$), and the difference between reactor and jacket temperatures ($\Delta T_{RJ}$) are recorded by a LabVIEW program every 0.6 s.

The calorimetric device was combined via an ATR-Dipper with an Equinox 55 FT-IR spectrometer from Bruker. The dipper system was obtained from Axiom. The ATR crystal is made of diamond, which combines the advantage of chemical inertness with the disadvantage of a diamond vibrational band in the area of 2700−1700 $cm^{-1}$. This means a reduced amount of data because a lot of typical absorbance bands are not visible. On the other hand, the complete fingerprint area can be used even with high concentrations because the pathway of the IR beam in the reaction system is extremely short, only some $\mu$m.

**Determination of Device-Specific Heat Flow Parameters.** As with most commercial calorimeters, the one presented here also measures only one heat flow during an experiment. For an isothermal experiment this would have no further consequences if the heat produced by the chemical reaction would be the only heat flow that varies over time. All of the other heat flows could then be taken into account by subtracting the baseline. However, in many cases the heat transfer coefficients will change during the chemical reaction because, for example, the viscosity of the reaction mixture varies. Therefore, the single heat flow measured is influenced by two processes varying over time: (i) the heat of reaction and (ii) the changing heat flow out of the reactor into the

(3) Leonhardt, J. *Thermokinetische Messverfahren im Vergleich*; Wissenschaft und Technik Verlag: Berlin, 1997.
(4) (a) Köhler, W.; Riedel, O.; Scherer, H. *Chem. Ing. Tech.* **1972**, *44*, 1216. (b) Schildknecht, J. *Thermochim. Acta* **1981**, *49*, 87.
(5) VDI. *VDI-Wärmeatlas, V. Wärmeübergang in Rührkesseln*, 4th ed.; VDI−Verlag: Düsseldorf, 1984.
(6) Zogg, M. *Einführung in die Mechanische Verfahrenstechnik*, 3rd ed.; Teubner: Stuttgart, 1987.

***Table 1.*** **Calibration Model Describing the Heat Flows Occurring in the Experimental Device in the Absence of a Chemical Reaction**

| | |
|---|---|
| $0 = q_{comp} - q_{flow} - q_{loss} + q_{stir}$ (1) | heat flow balance<br>$q_{comp}$: compensation heating [W]<br>$q_{flow}$: heat flow into the jacket [W]<br>$q_{loss}$: heat loss through the IR dipper [W]<br>$q_{stir}$: heat flow due to stirring [W] |
| $q_{loss} = \frac{1}{\frac{1}{\alpha_r A_{dipper}} + \boldsymbol{P_1}}(T_R - T_{dipper})$ (2) | heat loss through the IR dipper<br>$T_{dipper}$: temperature of the dipper [K]<br>$A_{dipper}$: dipper cross section [m$^2$]<br>$\alpha_r$: reactor−sided heat transfer coefficient [W/K/m$^2$]<br>$\boldsymbol{P_1}$: parameter to be fitted [m$^2$ K/W] |
| $q_{flow} = \frac{1}{\frac{1}{\alpha_r} + P_J} A_w (T_R - T_J)$ (3) | heat flow into the jacket<br>$T_R$: reactor temperature [K]<br>$T_J$: jacket temperature [K]<br>$\alpha_r$: reactor−sided heat transfer coefficient [W/K/m$^2$]<br>$A_W$: wetted wall area [m$^2$]<br>$\boldsymbol{P_J}$: function of $T_J$ [m$^2$ K/W] |
| $\alpha_r = \lambda \cdot d_B^{-1} \cdot 1.4 \cdot Re^{2/3} \cdot Pr^{1/3} \cdot \left(\frac{\eta_{fl}}{\eta_w}\right)^{0.14} \cdot \left(\frac{d_R}{d_B}\right)^{-0.3} \cdot \left(\frac{h}{d_B}\right)^{0.45} \cdot \left(\frac{h_R}{h_F}\right)^{0.2} \cdot \left(\frac{h_F}{d_B}\right)^{-0.6} \sin(\gamma)^{0.5} Z^{0.2}$ (4) | equation to determine the reactor-sided heat transfer coefficient; for notation see ref 5 |
| $P_J = e^{(\boldsymbol{P_{j-1}} \cdot T_J)} \boldsymbol{P_{j-2}} + \boldsymbol{P_{j-3}}$ (5) | $P_J$ is a function of the jacket temperature $T_J$<br>$\boldsymbol{P_{j-1}} - \boldsymbol{P_{j-3}}$: parameters to be fitted. |
| $q_{stir} = \boldsymbol{P_s} \rho n^3$ (6) | heat flow due to stirring<br>equation from ref 6<br>$n$: speed of the stirrer [1/s]<br>$q_{stir}$: heat flow due to stirring [W]<br>$\boldsymbol{P_s}$: parameter to be fitted |

cooling jacket. To be able to take the changing heat transfer coefficients into account, the device-specific heat flow parameters have to be determined. Such a calibration has only to be done once and can then be applied to all following reaction measurements.

The measurements for the calibration were carried out at steady-state conditions. The power signal of the heater ($q_{comp}$) was determined at different settings of jacket temperature ($T_J$) and difference between jacket and reactor temperature ($\Delta T_{RJ}$). The stirrer speed was kept constant at 750 rpm during the calibration and the later reaction measurements. Toluene and water were used as calibration fluids. The calibration surface ($q_{comp}$ vs $T_J$ vs $\Delta T_{RJ}$) obtained for toluene is shown in Figure 2.

The equations given in Table 1 describe the different heat flows shown in Figure 1 (ignoring $q_{react}$) and considered in the calibration model:

Equation 1 describes the heat flow balance in the calorimeter.

Equation 2 describes the heat loss through the IR-Dipper. This correction is necessary because the dipper tube is made of hastelloy steel, which is a good heat conductor. To establish constant conditions, the outside temperature of the dipper was controlled and kept constant at 313 K (= $T_{Dipper}$).

Equation 3 describes the heat flow through the reactor wall into the cooling fluid of the jacket. The overall heat transfer coefficient can be divided into several parts. One part, depending on the content of the reactor, is described by $\alpha_r$, the reactor-sided heat transfer coefficient. For the calibration liquids, $\alpha_r$ was calculated according to eq 4. The

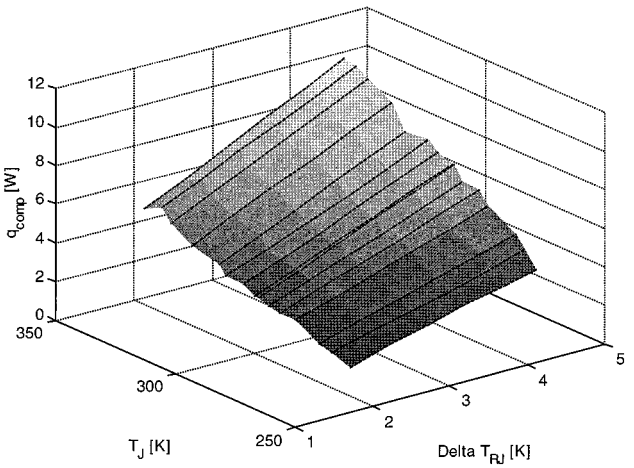


***Figure 2.*** **Thermal calibration of device using toluene: Surface of compensation power ($q_{comp}$) measured for different jacket temperatures ($T_J$) and temperature differences between reactor and jacket ($\Delta T_{RJ}$).**

second part, accounting for the thermal conductivity and thickness of the wall as well as for the jacket-sided heat transfer coefficient, is described by the function $P_J$ ($T_J$, $\boldsymbol{P_{j-1}}$, $\boldsymbol{P_{j-2}}$, $\boldsymbol{P_{j-3}}$) given in eq 5, in which the parameters $\boldsymbol{P_{j-1}}$, $\boldsymbol{P_{j-2}}$, and $\boldsymbol{P_{j-3}}$ have to be fitted. The parameter $P_J$ depends on the temperature in the jacket, due to for example the temperature dependence of the viscosity of the cooling fluid.

Equation 6 describes the heat flow due to stirring.

Other terms such as the heat of vaporization were neglected in the heat balance because for the applied temperature ranges and duration of the experiments solvent

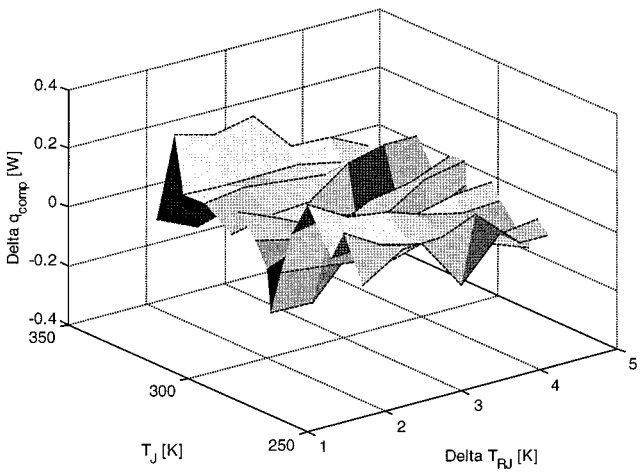


***Figure 3.*** **Thermal calibration of device using toluene: Difference between measured (see Figure 2) and simulated (see eqs 1−6 in Table 1) compensation power ($\Delta q_{comp}$) measured for different jacket temperatures ($T_J$) and temperature differences between reactor and jacket ($\Delta T_{RJ}$).**

vaporization and condensation at the lid were negligible.

The parameters $P_l$, $P_{j\_1}$, $P_{j\_2}$, $P_{j\_3}$, and $P_s$ of the model given in Table 1 were fitted using the measured values shown in Figure 2. The fitting procedure was performed using the Optimization Toolbox in MATLAB. The finally resulting deviations between the fitted model and the calibration measurements were in the range of 2−4% (Figure 3). The two calibrations obtained with toluene and water agreed well. The heat flow due to stirring was neglected for further evaluations because for $P_s$ in all cases very small values were obtained. The stability of the results was checked by varying the initial values of the parameters to be fitted.

**Experimental Procedure for Determining Reaction Parameters.** Due to the sensitivity towards changes in temperature, isothermal experiments are strictly preferred in combination with FT-IR analysis. The experiments were performed in the semibatch mode. The solvent and one of the reactants were filled into the calorimeter, and the experimental temperature as well as the temperature difference between reactor and jacket temperature were set by the LabVIEW software. After allowing 30 min for thermal equilibration, dosing was started using a syringe pump. To keep the dosing time as short as possible, the feed rate was set to a maximum value such that the PID-controller could still maintain a constant temperature. In the work presented, dosing was performed at a rate of 1 mL/min.

First, an IR measurement was done to obtain a background spectrum. Then, the time-resolved IR measurement was started. The FT-IR spectra were taken every 50 s, and 40 scans each were sampled to generate one spectrum with a resolution of 2 $cm^{-1}$ using the Chrom software from Bruker. The duration of the experiments from the beginning of dosing until termination was about 150 to 250 min depending on the experimental temperature.

During early phases of process design, any additional experiment means a significant burden. Thus, to avoid the measurement of parameters required for an exact modeling of the dosing period (i.e., the temperature and heat capacity of the feed, mixing enthalpies), the power signal during dosing was omitted for the parameter fitting. Nevertheless, the simulation of the reactor included this period because it is important for the correct determination of the reaction parameters. Contrary, for the evaluation of the spectra, measurements recorded during the dosing period were considered.

**Model Reaction.** We used the reaction of butan-2-ol (**1**) with isocyanatobenzene (**2**) to phenyl-carbamic acid *sec*-butylester (**3**) conducted in toluene to test the new calorimeter and evaluation procedure:

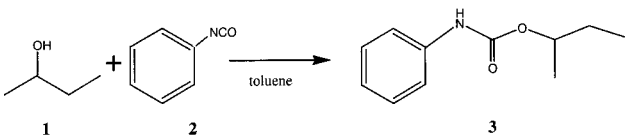


The reaction is described well in the literature[3] and the reaction parameters are known.

The molar ratio **1** to **2** was varied between 0.5 and 3.5. The concentrations **1** and **2** were varied in the ranges from 1.5 to 5.5 mol/L and 1 to 4 mol/L, respectively. The reaction kinetics have been described using the Arrhenius approach:[3]

$$\frac{dc_3}{dt} = k(T_R)c_1^{\beta 1}c_2^{\beta 2} = k_0\, e^{-(E_a/RT_R)}c_1^{\beta 1}c_2^{\beta 2} \qquad (7)$$

where $c_1$, $c_2$, and $c_3$ are the concentrations of **1**, **2**, and **3**, respectively, $t$ is time, $k_0$ is the frequency factor [L/mol/s], $E_a$ is the activation energy [J/mol], and $\beta 1$ and $\beta 2$ are the reaction orders of **1** and **2**, respectively. The reaction has been reported to be of second order, every reactant in the kinetic law having an order of one.[3] The reaction is definite and homogeneous. In a wide range of temperatures the reaction provides heat release rates that are sufficiently high for the resolution used. In total 33 experiments with 10 different initial concentrations of the reactants have been performed. The reactor temperature was varied from 272 to 342 K in intervals of 5 K. Reproducibility was checked by conducting five experiments at 327 K and identical concentrations.

For the experiments we used Fluka and Merck KGaA pro analysi quality chemicals, compound **2** was of ≥98% purity. We did not work under strictly water free conditions. Compound **2** was dosed to the mixture of **1** and toluene because it is the more reactive chemical. It was checked by NMR measurements that no unwanted side reactions proceeded like the reaction of water with **2**.

**Evaluation of the Thermal Signal Recorded in Reaction Measurements.** As data pretreatment for the thermal signal (compensation power readings), we first applied a low pass filtering using MATLAB and then re-sampled the filtered data to reduce the number of measurement points. Data pretreatment was applied to increase the performance of the following fitting procedure.

When a reaction is proceeding, a corresponding term $q_{react}$ [W] has to be added to the heat balance given in Table 1:

$$0 = q_{comp} - q_{flow} - q_{loss} + q_{stir} - q_{react} \qquad (8)$$

where $q_{react}$ can be described by the following equations in

which both $\beta 1$ and $\beta 2$ of eq 7 are set equal to one:

$$q_{\text{react}} = \frac{\mathrm{d}n_3}{\mathrm{d}t} \cdot \Delta H_{\text{R}} \tag{9}$$

$$\frac{\mathrm{d}n_3}{\mathrm{d}t} = k(T_{\text{R}}) c_1^1 c_2^1 V_{\text{R}} \tag{10}$$

$$c_1 = \frac{n_1}{V_{\text{R}}} \tag{11}$$

$$c_2 = \frac{n_2}{V_{\text{R}}} \tag{12}$$

$$V_{\text{R}} = V_0 + \upsilon t \quad \text{during dosing} \tag{13a}$$

$$V_{\text{R}} = \text{const} \quad \text{after dosing} \tag{13b}$$

$$\frac{\mathrm{d}n_1}{\mathrm{d}t} = -\frac{\mathrm{d}n_3}{\mathrm{d}t} \tag{14}$$

$$\frac{\mathrm{d}n_2}{\mathrm{d}t} = -\frac{\mathrm{d}n_3}{\mathrm{d}t} + \frac{\mathrm{v}\rho_2}{M_2} \quad \text{during dosing} \tag{15a}$$

$$\frac{\mathrm{d}n_2}{\mathrm{d}t} = -\frac{\mathrm{d}n_3}{\mathrm{d}t} \quad \text{after dosing} \tag{15b}$$

where $n_1$, $n_2$, *and* $n_3$ are the number of moles of **1**, **2**, and **3**, respectively, $\Delta H_{\text{R}}$ is the heat of reaction [J/mol], $V_{\text{R}}$ is the volume [L] of the reaction mass at time $t$, $V_0$ is the volume [L] at time zero, $\upsilon$ is the dosing rate [L/s], and $\rho_2$ and $M_2$ are the density [g/L] and molar mass [g/mol] of **2**, respectively.

As calibration is already done, the unknown reaction parameters in the model are now $\Delta H_{\text{R}}$ and $k(T_{\text{R}})$. The reactor-sided heat transfer coefficient $\alpha_{\text{r}}$, which is included in $q_{\text{loss}}$ and $q_{\text{flow}}$ (see eqs 2 and 3), is also unknown, because the physical properties of the reaction mixture are of course not equal to the properties of the calibration liquids. This parameter was dissected into a constant value describing the heat transfer before dosing is started, a value describing the change during dosing, and a value depending on the conversion of the reaction.

Using the already calibrated device parameters, the reaction parameters $\Delta H_{\text{R}}$ and $k$, as well as the three values describing the reactor-sided heat transfer were fitted to the measurements obtained for various initial concentrations and temperatures. The fitting procedure was implemented using ACSL, and seven different initial parameter sets were used for fitting each experiment. The $k(T_{\text{R}})$ values were determined as average over the results obtained for the seven initial values, while $\Delta H_{\text{R}}$ was determined as average over all 33 experiments (and seven initial values each). The resulting $k(T_{\text{R}})$ values were plotted in an Arrhenius plot to obtain the $E_{\text{a}}$ and $k_0$ by curve fitting.

**Evaluation of FT-IR Measurements.** Also the time-resolved FT-IR signals were evaluated by parameter fitting for determining kinetic rate constants assuming that Lambert Beer's law is strictly fulfilled. Four wavenumbers (1540, 1443, 1224, and 1053 $\text{cm}^{-1}$) belonging to the spectra of the product **3** were selected. The basis of the fitting without

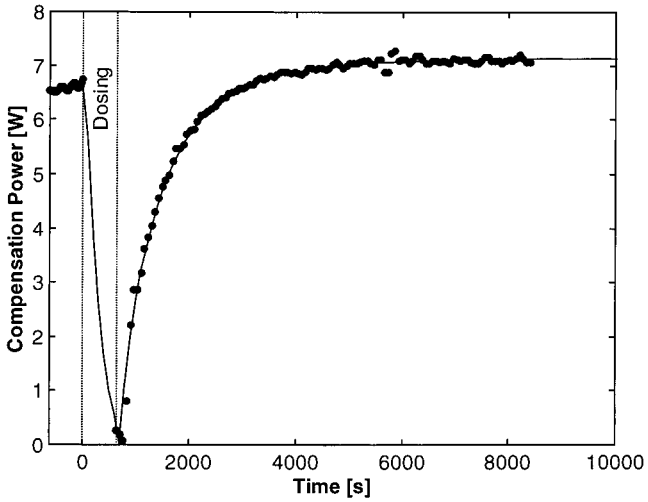


***Figure 4.*** **Evaluation of the calorimetric data: Measured signal of one of the 33 experiments (317 K) after filtering (black dots) as well as fitted model curve (black line). Data recorded during dosing procedure (indicated by two vertical lines) are not used for fitting.**

calibration is the Lambert Beer's Law:

$$A = \epsilon(\nu) l(\nu) \cdot \frac{n_3}{V_{\text{R}}} \tag{16}$$

where $A$ is absorbance, $\epsilon(\nu)$ is the absorption coefficient, and $l(\nu)$ is the thickness of the medium in which the absorption is proceeding. Both $\epsilon$ and $l$ are dependent on the wavenumber, but because they are constant for a given wavenumber, they can be combined to one factor. Equations 10−15 complete the reactor model used for evaluating the FT-IR measurements.

The absorbance-time curves at selected wavenumbers were normalized using the maximum absorbance value recorded for a given wavenumber. Using numerical algorithms, concentration−time curves for the product were calculated. These were normalized analogous to the measured absorbance-time curves. In the evaluation procedure realized in MATLAB, the calculated relative concentration−time curves were fitted to the measured relative absorbance-time curves by varying $k(T_{\text{R}})$. Thus, four different values of $k$ (one for each wavenumber) were obtained for each of the 33 experiments. Arrhenius fits were done for the four wavenumbers separately as well as for all values of $k$ together. As for the calorimetric measurements, also in the evaluation of the FT-IR measurements observation of a reaction until 100% conversion is not required because parameter fitting is applied.

## Results and Discussion

**Calorimetry.** As an example, Figure 4 shows that the reactor is in thermal equilibrium before dosing is started. When dosing starts, the PID-controller reduces the power of the compensation heating to keep $T_{\text{R}}$ strictly constant (the maximum temperature deviation recorded during all experiments was 0.3 K). As explained above, the data points recorded during dosing were omitted for the parameter fitting (and therefore are not shown in Figure 4), while the

***Table 2.*** **Reaction Parameters Obtained for the Model Reaction as well as Comparison to Literature Values[a]**

| | power compensation calorimeter | FT-IR: fit to absorbance values | literature[3]: several methods[f] |
|---|---|---|---|
| $E_a$ [kJ/mol] | $33 \pm 1$[b] | $40 \pm 1$[b] | 41 (39−44) |
| $k_0$ [L/mol/s] | $96 \pm 1$[b] | $1200 \pm 230$[b] | 1800 (1400−2100) |
| $k$ (327 K) [L/mol/s] | 5.0E−4 ± 1E−5[c] | 5.9E−4 ± 2E−5[e] | 5.1E−4[g] |
| $-\Delta H_R$ [kJ/mol] | $93 \pm 19$[d] | − | 85 (82−90) |

[a] See text for further explanation on derivation of standard deviations. The term "initial values" refers to the different start values used in the fitting procedure. [b] Standard error obtained from least square fitting (Arrhenius plot). [c] Standard deviation obtained for results from five replicate experiments and seven different initial values each. [d] Standard deviation obtained for results from all 33 experiments and seven different initial values each. [e] Standard deviation obtained for results from five replicate experiments using the wavenumber 1540 $cm^{-1}$. [f] Mean values as well as minimum and maximum values (in brackets) obtained from different methods. [g] Calculated from mean values for $k_0$ and $E_a$.

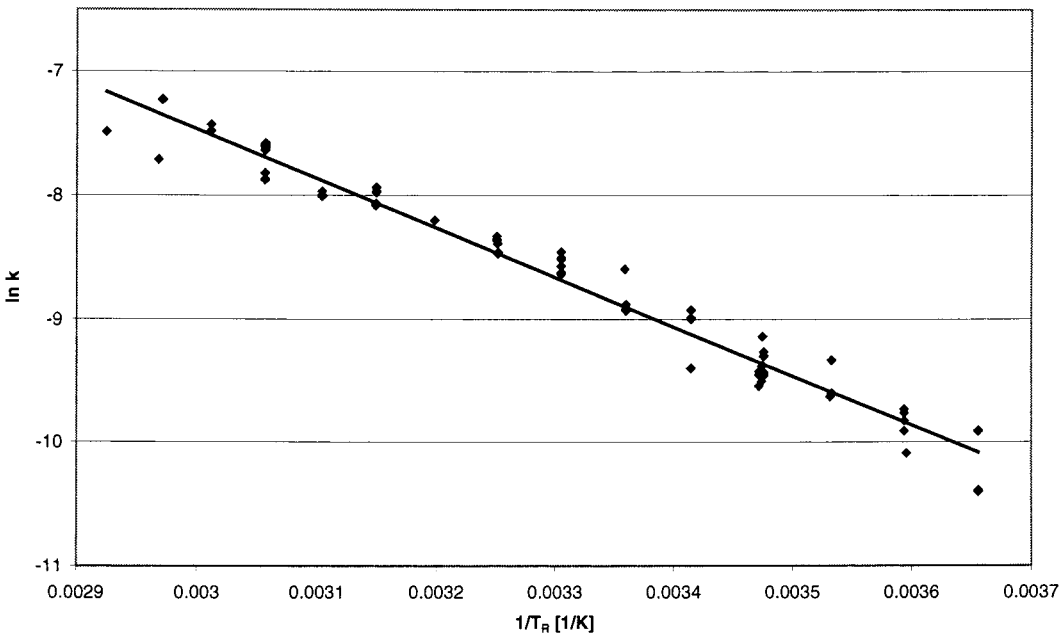


***Figure 5.*** **Evaluation of the calorimetric data: Arrhenius plot of the fitted kinetic rate constants for the determination of $k_0$ and $E_a$. The data points represent 33 experiments for which each 7 initial values were used in the fitting procedure. The numerical values obtained are given in Table 2.**

simulation of the reactor also included this period. Although this procedure means that less data are available, it is feasible because not the concept of thermal conversion was used for determining the reaction parameters but instead parameter fitting was applied.

When the principle of thermal conversion is applied, the area under the baseline of a calorimetric signal is integrated to obtain the heat of reaction. For this procedure almost complete conversion must be observed. Contrary, in the present work from the 33 measurements used for determining the heat of reaction only the measurements at temperatures above 313 K were conducted until almost 100% conversion was reached. All other experiments were stopped at a conversion of about 90%.

As an example, Figure 4 shows that the fit of the reaction model agrees well with the power compensation signal recorded. The average deviation for determining $k(T_R)$ and $\Delta H_R$ from a single experiment using different initial values of the parameters to be fitted is 7 and 6%, respectively. These deviations result mainly from the fact that the three heat transfer parameters have to be fitted as well, thus, resulting in nonuniqueness of the optimization problem. When for the determination of $\Delta H_R$ one set of initial parameters was used for evaluating all experiments, a mean deviation over seven sets of initial parameters of 20% was obtained. Similarly, a three times higher average deviation was obtained for the evaluation of $k(T_R)$ and $\Delta H_R$ from five replicate experiments conducted at 327 K and identical concentrations when the experimental effects on the results were considered in addition to the purely numerical ones. The overall variability in determining these two parameters from replicate experiments is 2% for $k(T_R)$ and 4% for $\Delta H_R$, thus showing a high reproducibility of the approach.

The value obtained for $\Delta H_R$ agrees well with the one reported in the literature (Table 2). It is important to mention that the literature values referenced in Table 2 are average values obtained from calorimetric measurements done in isothermal, isoperibol, adiabatic, as well as temperature-programmed measurements.[3]

The $k(T_R)$ values fitted for the 33 experiments are shown in an Arrhenius plot in Figure 5. The values of $k_0$ and $E_a$ fitted to these data are somewhat different than those reported

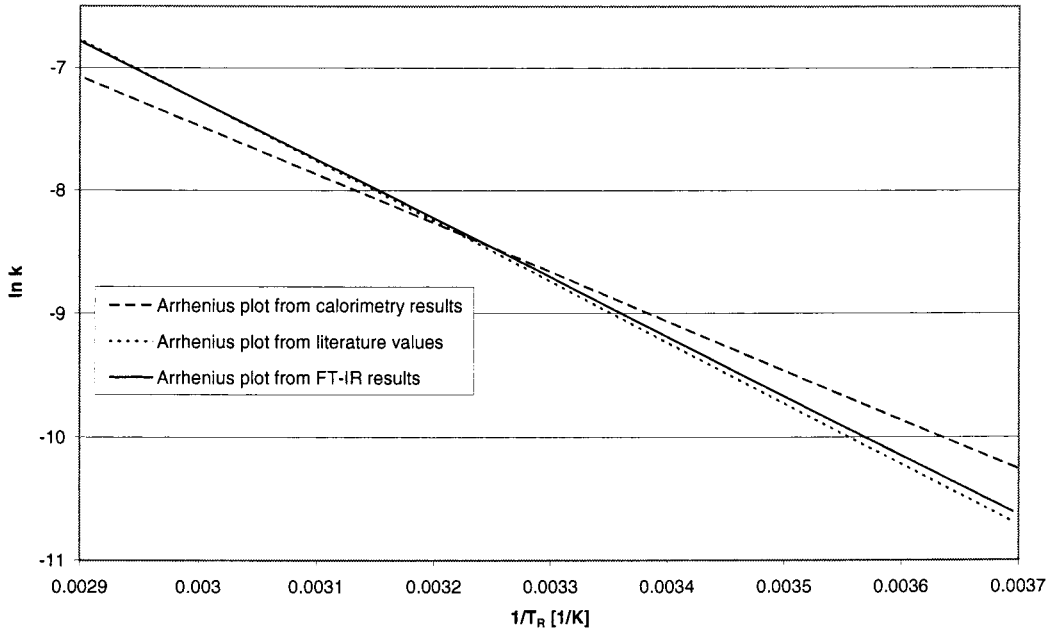


***Figure 6.*** **Comparison of Arrhenius plots obtained from the calorimetric as well as from the FT-IR data with results reported in the literature.[3] The numerical values obtained are given in Table 2.**

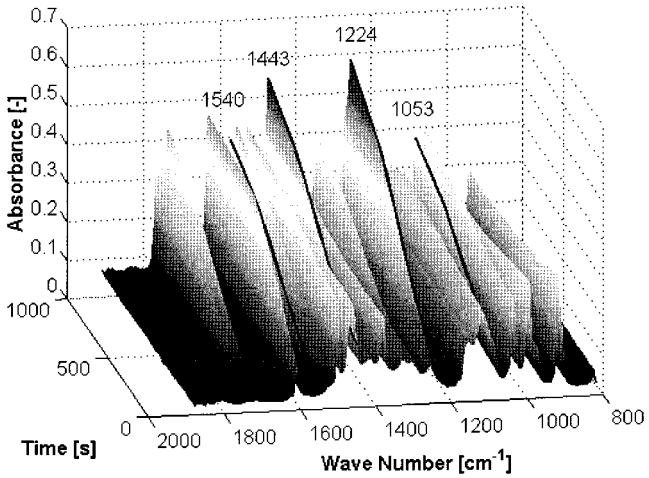


***Figure 7.*** **Section of the time-resolved absorbance spectra obtained at 317 K. Growing bands represent the increasing amount of product. The wavenumbers marked by black lines were used for the fitting procedure.**

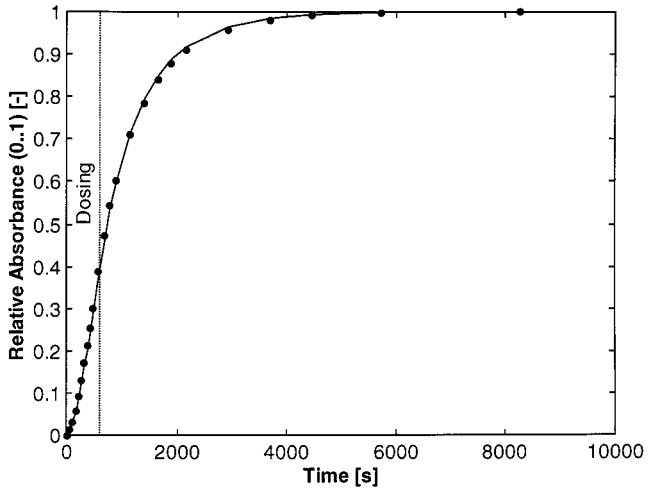


***Figure 8.*** **Plot of the relative absorbance recorded at 317 K and 1540 cm$^{-1}$ versus time: Points represent the measured and normalized absorbance, while the line represents the fitted model curve. All data including those sampled during dosing are used in the fitting procedure.**

in the literature (Table 2), but in the investigated temperature range (272−342 K) the resulting $k(T_R)$ have the same order of magnitude as can be seen from Figure 6. The general applicability of the Arrhenius model is demonstrated by a value of $r^2$ of 0.97.

**FT-IR Measurements.** In Figure 7 a section of the time-resolved FT-IR spectra is shown, in which the four wavenumbers used for evaluation are marked by black lines. The fit of the kinetic model to the absorbance at 317 K and 1540 cm$^{-1}$ is shown in Figure 8. A good agreement between measurements and simulation was obtained in this as well as in all other cases. Unlike the calorimetric evaluation, here the fitting is done for the whole semibatch.

The fitting results derived from the FT-IR measurements are shown in Figure 9 as well as in Table 2. The Arrhenius plot in Figure 9 shows the values for the kinetic rate constants resulting from the mentioned fit procedure. These values agree well for the four wavenumbers and a given temperature because they all represent the concentration of the same product molecule. Consequently, also the values obtained for $k_0$ and $E_a$ and the different wavenumbers agree well as shown by the curves in Figure 9. Therefore, in a final step $k_0$ and $E_a$ were determined from fitting all $k$ values obtained for the four wavenumbers together (Table 2). The resulting values of $k_0$ and $E_a$ result in $k(T_R)$ values that agree well with the results reported in the literature (Figure 6). The value for $k$ (54 °C) agrees well with that obtained from calorimetry and literature results (Table 2). A value for $r^2$ of 0.98 again supports the applicability of the Arrhenius law. As already discussed, the FT-IR cannot give the reaction enthalpy like the calorimetric measurement.

To ensure that only bands of the product were used, FT-IR spectra of the pure components were taken (Figure 10).

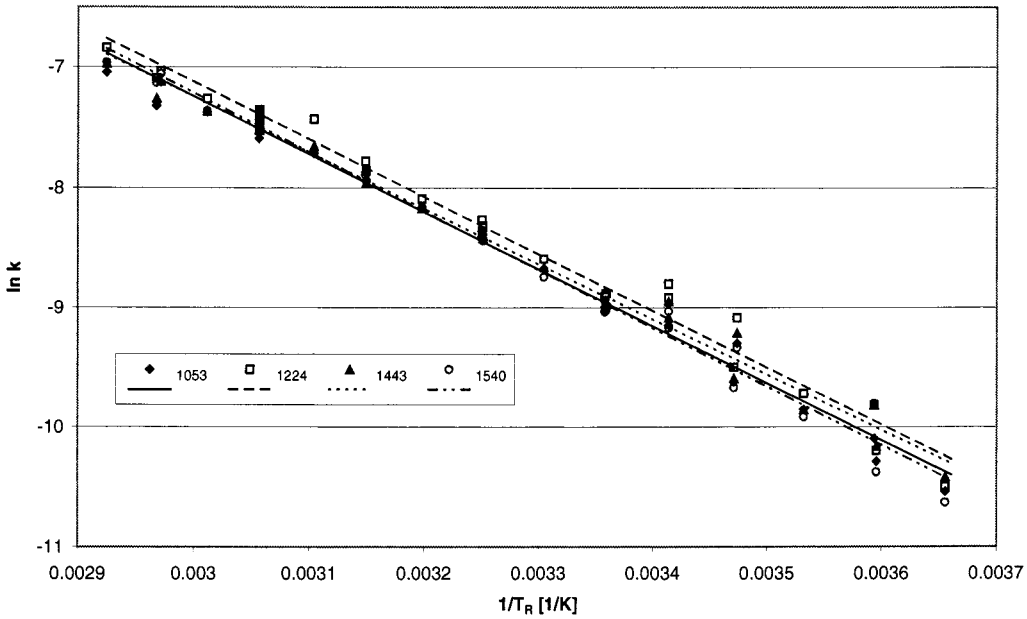


***Figure 9.*** **Evaluation of the FT-IR data: Arrhenius plots of the fitted kinetic rate constants determined from the four wavenumbers indicated in Figure 7. Symbols represent measurements, and lines, the corresponding Arrhenius fits. The values resulting from fitting the *k* values obtained for all four wavenumbers together are given in Table 2.**

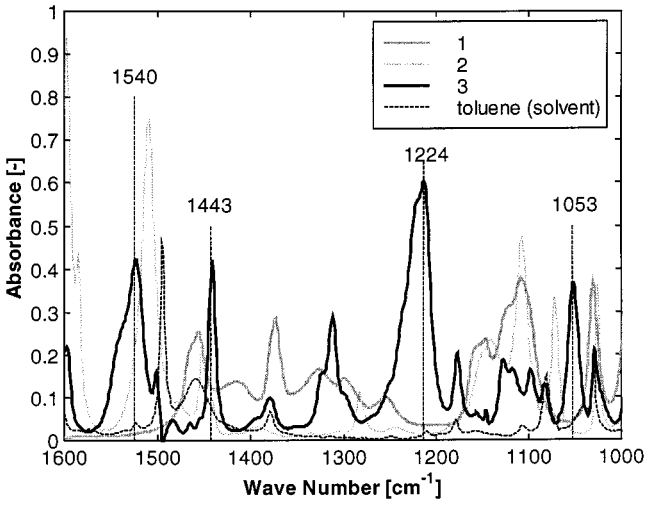


***Figure 10.*** **Absorbance spectra of the pure components.**

When discussing Figure 10, one has to be aware of the fact that the relative absorbance between the various species is altered as compared to the reaction mixture, where the concentrations are different. The mixture might have slightly shifted absorbance bands due to the presence of hydrogen bonds.

In this work wavenumbers unique to a single compound could be identified and were used for the evaluation of the kinetic parameters. For each wavenumber a linear dependency between absorbance and concentration of the product was assumed (eq 10) so that the rate constants could be obtained by direct fitting. We are aware of the fact that not in all cases a sufficient number of unique wavenumbers can be identified to make a direct fit. In these cases more sophisticated chemometric and factor analytical techniques have to be applied to obtain the reaction parameters from the FT-IR measurements.

## Summary and Conclusions

In our work we were able to show that it is possible to work with a small calorimetric device which can provide augmented information by the use of an additional on-line measurement technique (FT-IR in our case). Reproducible measurements were obtained with both the calorimetric and the FT-IR technique, and the resulting reaction parameters are in good agreement with literature values. Thus, the feasibility of the whole approach (small device, parameter fitting instead of principle of thermal conversion, combined measurements) was shown with a simple model reaction.

Crucial constants during process development are the amount of reactants and the time needed to perform experiments. Considering that a standard reaction calorimeter with FT-IR is 10−40 times larger than the one presented, during the development phase of a new process many more experiments could be done with the same mass of reactants if the smaller device is used. We used the same quantity of chemicals for 33 measurements than one experiment in a standard calorimeter with a volume of 1.5 l would have needed.

By applying parameter fitting for the evaluation of the thermal signal, the time needed to perform experiments can be shortened significantly, because complete conversion of the reactants is not required (most of the experiments were stopped at about 90% conversion). With the conventional calorimetric assessment (based on the principle of thermal conversion) the experiments can only be shortened when the conversion at the end of the experiment is determined by another analytical technique such as gaschromatography. Furthermore, for the new procedure the temperature and heat capacity of the feed as well as mixing enthalpies have not to be determined.

In the approach presented additional information is provided by online spectroscopic measurements. For the simple reaction investigated in this work, reaction parameters could be obtained from each measurement technique separately. For more complex reactions the combined evaluation of the two sources of information will be required.

Due to the fact that more experiments can be performed, more possible working conditions of a reactor can be tested in detail so that at the end of the development phase much more knowledge would be available. In summary, the new device presented in this paper is a valuable tool for determining reaction parameters in early stages of process development.


## Acknowledgment

We thank Dr. P. Skrabal and Dr. O. Kut for comments on the manuscript and F. Mayer, P. Steiner, H. P. Schläpfer, and M. Wohlwend for technical support.

Received for review July 3, 2000.

OP000072A